# Strong magnetic coupling of spins in Fe(II) dimers with differently charged thioindigo ligands

| | |
|---|---|
| Journal: | *Dalton Transactions* |
| Manuscript ID | DT-COM-04-2020-001262.R1 |
| Article Type: | Communication |
| Date Submitted by the Author: | 18-May-2020 |
| Complete List of Authors: | Konarev, Dmitri; Institute of Problems of Chemical Physics RAS,<br>Kuz`min, Alexey; Institute of Solid State Physics RAS,<br>Batov, Mikhail; Moscow State University,<br>Khasanov, Salavat; Institute of Solid State Physics RAS,<br>Otsuka, Akihiro; Kyoto University - Yoshida Campus, Department of Chemistry; Research Center for Low Temperature and Materials Sciences<br>Yamochi, Hideki; Kyoto University, Division of Chemistry in Graduate School of Science<br>Kitagawa, Hiroshi; Kyoto University, Department of Chemistry<br>Lyubovskaya, Rimma; Institute of Problems of Chemical Physics RAS, |
| | |

COMMUNICATION

# Strong magnetic coupling of spins in Fe(II) dimers with differently charged thioindigo ligands

Received 00th January 20xx,
Accepted 00th January 20xx

DOI: 10.1039/x0xx00000x

Dmitri V. Konarev, *[a] Alexey V. Kuzmin,[b] Mikhail S. Batov,[a,c] Salavat S. Khasanov,[b] Akihiro Otsuka,[d, e] Hideki Yamochi,[d, e] Hiroshi Kitagawa[d] and Rimma N. Lyubovskaya[a]

**First coordination $\{Crypt[2.2.2](K^+)\}_2\{Fe^{II}(TI^{\bullet-})(TI^{2-})\}_2 \cdot 2C_6H_4Cl_2$ (1) complex of iron(II) containing radical anions and dianions of thioindigo (TI) was obtained. Complex has two high-spin $Fe^{II}$ centers bound by two oxygen atoms and the $TI^{\bullet-}$ radical anions are coordinated to each $Fe^{II}$. As a result, the the 4-spin system consisting of $TI^{\bullet-}$ ($S$ = 1/2) - $Fe^{II}$ ($S$ = 2) - $Fe^{II}$ ($S$ = 2) - $TI^{\bullet-}$ ($S$ =1/2) coupled spins is formed within a dimer with strong $Fe^{II}$- $Fe^{II}$ ($J/k_B$ = –51.1 cm$^{-1}$) and weaker $Fe^{II}$ - $TI^{\bullet-}$ interactions of $J/k_B$ = –35.4 cm$^{-1}$.**

Organic dyes are used not only as colorants[1] for clothes but can also serve as electronic materials, photoconductors[2] and yield transition metal complexes[3]. For example, indigo forms complexes with one or two transition metals in its deprotonated state.[3a-3e] Indigo and related thioindigo (Scheme 1) can change conformation from *trans*- to *cis*- under reduction allowing coordination of both oxygen atoms to metal centers[3f-3i]. Optical and magnetic properties of such coordination complexes can be modified corresponding to oxidation states of the ligands. Especially when they accommodate unpaired electrons, magnetic properties will be drastically modulated[3d]. It should be noted that complexes obtained till now with the indigo-type ligands contain mainly diamagnetic neutral dyes or dye anions[3] in spite of that both indigo and thioindigo (Scheme 1) can form radical anions under reduction in solution[4] or in solid state[3g, 5].

In this work we study $\{Cryptand(K^+)\}_2\{Fe^{II}(TI^{\bullet-})(TI^{2-})\}_2 \cdot 2C_6H_4Cl_2$ (**1**) complex between thioindigo (TI) anions and $Fe^{II}$ cations. In this complex, each metal center coordinates two differently charged TI ligands in *cis*-conformation (Scheme 1), and these units are bound to form dimers through the $\mu^2$-oxygen bridges. This is the first coordination complex containing only dye ligands of one type since previously only mixed ligand complexes with such dyes were obtained[3]. Molecular structure, optical, and magnetic properties of **1** are discussed. Unusually strong magnetic coupling is observed between two $Fe^{II}$ centers ($S$ = 2). Paramagnetic $TI^{\bullet-}$ radical anions ($S$ = 1/2) additionally coordinate to the $Fe^{II}$ centers and are involved in this coupling forming the $TI^{\bullet-}$ - $Fe^{II}$ - $Fe^{II}$ - $TI^{\bullet-}$ magnetic chains.

Scheme 1.

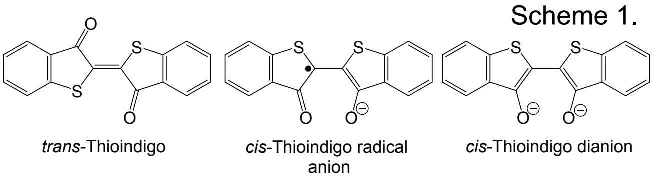

Synthesis of **1** was carried out by the interaction of chemically generated salt $\{cryptand(K^+)\}(TI^{\bullet-})$ with $Fe_3(CO)_{12}$ at a 2:1 molar ratio. $\{Cryptand(K^+)\}(TI^{\bullet-})$ was obtained by the reduction of pristine TI with potassium graphite in the presence of one equivalent of cryptand to form red-violet solution. Addition of this salt to $Fe_3(CO)_{12}$ yields brown solution from which the crystals of $\{cryptand(K^+)\}_2\{Fe^{II}(TI^{\bullet-})(TI^{2-})\}_2 \cdot 2C_6H_4Cl_2$ (**1**) were obtained under slow mixing with *n*-hexane. It can be concluded from the analysis of magnetic behavior of **1** that $Fe^{II}$ is formed (magnetic behavior of **1** is presented below). The formation of $Fe^{II}$ is understood as the result of electron transfer from $Fe^0$ to $TI^{\bullet-}$ represented as $Fe^0 + 2(TI^{\bullet-}) \rightarrow Fe^{II} + 2(TI^{2-})$. The mixture of $Fe^{II}$, $TI^{\bullet-}$ and $TI^{2-}$ ions is formed from which complex **1** crystallizes as pure phase by slow mixing with *n*-hexane. Interaction of pristine TI with $Fe_3(CO)_{12}$ provides no crystalline products.

There are two $\{Crypt[2.2.2](K^+)\}$ cations per $\{Fe^{II}(TI^{\bullet-})(TI^{2-})\}_2$ dimer in **1** indicating that dimer has dianion state, and each $Fe(TI)_2$ unit correspondingly has monoanionic state. Depending on charge distribution between the components, various kinds of combinations are possible such as $\{Fe^0(TI^0)(TI^{\bullet-})\}^-$, $\{Fe^I(TI^{\bullet-})_2\}^-$, $\{Fe^{II}(TI^{\bullet-})(TI^{2-})\}^-$ or $\{Fe^{III}(TI^{2-})_2\}^-$. To clarify acceptable ionization patterns, all optical, magnetic and structural data was examined. EPR data are of particular importance since each charged state of Fe and TI has individual clear magnetic state to show characteristic EPR spectra.

IR and optical spectra of pristine *trans*-TI, reference compounds, and complex **1** are listed in Table S1 (Figs. S1 and S2) and Fig. 1, respectively. Position of the band of carbonyl C=O stretching vibrations for *trans*-TI is at 1657 cm$^{-1}$ (Fig. S1). This band is strongly red shifted (1586 cm$^{-1}$) and decreases in intensity in the spectrum of the $TI^{\bullet-}$ salt. In the spectrum of **1,** highest-energy absorption band of weak intensity is observed only at 1522 cm$^{-1}$. Probably reduction and formation of coordination bonds with iron affects essentially the C-O vibrations. Optical spectrum of **1** shows the band of TI at 370 nm and a broad band of relatively low

---

[a] *Institute of Problems of Chemical Physics RAS, Chernogolovka, Moscow region, 142432 Russia;*
[b] *Institute of Solid State Physics RAS, Chernogolovka, Moscow region, 142432 Russia;*
[c] *M. V. Lomonosov Moscow State University, Leninskie Gory, Moscow, 119991, Russia;*
[d] *Division of Chemistry, Graduate School of Science, Kyoto University, Sakyo-ku, Kyoto 606-8502, Japan;*
[e] *Research Center for Low Temperature and Materials Sciences, Kyoto University, Sakyo-ku, Kyoto 606-8501, Japan.*

Electronic Supplementary Information (ESI) available: experimental section, X-ray crystallography, IR spectra of **1** and reference compounds, crystal structure and magnetic data for **1**. See DOI: 10.1039/x0xx00000x intensity with maximum at 740 nm. The latter band extends up to 1100 nm (Fig. 1). It is seen that reduction and coordination to iron shifts the lowest energy band of pristine TI (541 nm) to red side. Similar red shift of the lowest energy TI band was also observed at the formation of $\{Cp^*Cr^{III}(TI^{2-})\}_2$ (Fig. 1)[3g]. According to calculations, broad bands observed in the coordination complexes of indigo and TI were attributed to charge transfer bands from metal to the dye ligand. For example, these bands are observed in the spectra of the $\{Cp^*Cr^{II}\,Cl(\textit{cis}\text{-Indigo})^0\}$ and $\{Cp^*Cr^{III}(TI^{2-})\}_2$ (Fig. 1) complexes at 820 (1002) and 594 nm, respectively[3f, g].

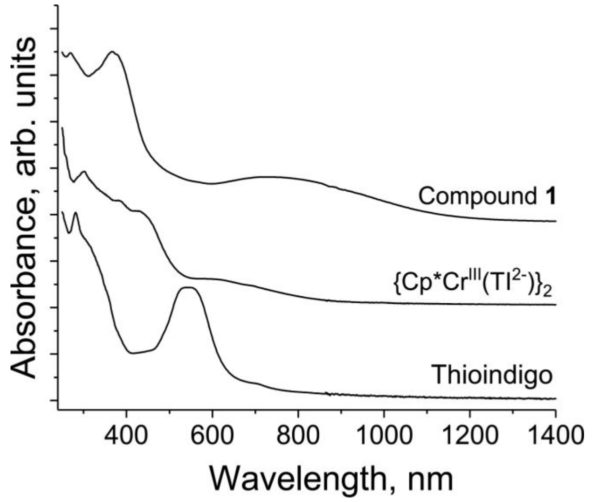

**Fig. 1** Experimental UV-visible-NIR spectra for pristine thioindigo (*trans*-form) measured in KBr pellets; coordination complex $\{Cp^*Cr^{III}(TI^{2-})\}_2$;[3g] and coordination complex **1** obtained in this work. Spectra of latter two complexes were measured in the anaerobic conditions.

Crystal structure of **1** was determined from X-ray diffraction at 120(2) K.‡ The system consists of two pairs of thioindigo species having different geometry which most probably can be attributed to TI with dianion and radical anion character, enclosing a cluster-like $[(\mu_2\text{-}O)_2Fe_2O_6]$ assembly formed by TI oxygens coordinated to iron(II) atoms. The distance between metal centers bridged by two oxygen atoms is 3.31 Å that is slightly longer as compared with previously reported chromium-containing dimer of thioindigo (3.13 Å)[3g].

Previously it was shown that pristine thioindigo has planar shape[6]. However, the population of LUMO at the reduction, which is antibonding for the central C=C bond, provides elongation of this bond and facilitates rotation of two halves of the molecule around this bond (see data for radical anions and dianions of TI in Table 1). As a result, the TI species attributed to the dianions have a rotation angle of two halves of the molecule around the central C-C bond of 31.16-31.79° indicating a single bond (Scheme 1) and nearly free rotation around this bond. Similar rotation is also possible for radical anions but this rotation is generally smaller in comparison with those for the dianions (14.33 and 19.19° in case of **1**). Radical anions can also have different length of the C=O and C(O)-C(=) bonds within one unit in accordance with Scheme 1. That is really observed for isolated *cis*-$TI^{\bullet-}$ radical anions in $\{Crypt(Na^+)\}(TI^{\bullet-})$[3g] (Table 1). Similar geometry is also observed for one of two $TI^{\bullet-}$ in **1** (Table 1). It should be noted that the difference between the length of the C=O and C(O)-C(=) bonds is also observed for the TI species attributed to the dianions in **1** and also for $\{Cp^*Cr^{III}(TI^{2-})\}_2$ (Table 1). But this difference can be attributed most probably to different coordination $\mu^2$- and $\mu$-modes for two oxygen atoms of TI. Expectedly, oxygen atom involved in the $\mu^2$-coordination forms longer C-O bond (Table 1).

Each iron atom forms four coordination bonds with oxygen atoms of two TI units and one oxygen atom of $TI^{2-}$ becomes a $\mu^2$-bridge between two iron atoms providing coordination number of five for iron atoms (Figs. 2 and S4). The average O(TI)-Fe bonds of 1.87-1.90 Å are short indicating effective coordination of TI oxygen atoms to iron. Only in case of the $\mu^2$-oxygen bridge, the lengths of the coordination bonds are elongated to 1.97-1.99 and 2.09-2.11 Å (Fig. 2 and Fig S4).

**Table 1.** Bond length (in Å) and angles (in °) in the thioindigo units in reference compounds and compound **1** studied in this work.

| Charge and conformation | Central C=C bond | C=O bonds | C(O)-C(=) bonds | Dihedral angle |
|---|---|---|---|---|
| Pristine neutral *trans*-TI[6] | 1.34(3) | 1.21(3) | 1.54(3) | 0 |
| *trans*-$TI^{\bullet-}$ in $\{Crypt(Na^+)\}(TI^{\bullet-})$[3g] | 1.411 (8) | 1.270(18)<br>1.34(3) | 1.356(15)<br>1.331(11) | 6.40 |
| *cis*-$TI^{\bullet-}$ in $\{Crypt(Na^+)\}(TI^{\bullet-})$[3g] | 1.411 (8) | 1.330(8)<br>1.377(12) | 1.305(12)<br>1.331(8) | 7.46 |
| *cis*-$TI^{2-}$ in $\{Cp^*Cr^{III}(TI^{2-})\}_2$ [3g] | 1.445(2) | 1.314(2)<br>1.351(2) | 1.384(2)<br>1.371(2) | 19.7 |
| *cis*-$TI^{\bullet-}$ in $\{Crypt(K^+)\}_2$ $\{Fe^{II}(TI^{\bullet-})(TI^{2-})\}_2$* | 1.448(5)<br>1.450(5) | 1.309(4)<br>1.336(4)<br>1.322(4)<br>1.328(4) | 1.393(5)<br>1.375(5)<br>1.382(5)<br>1.386(5) | 19.19<br>14.33 |
| *cis*-$TI^{2-}$ in $\{Crypt(K^+)\}_2$ $\{Fe^{II}(TI^{\bullet-})(TI^{2-})\}_2$* | 1.450(5)<br>1.444(5) | 1.332(4)<br>1.352(4)<br>1.327(4)<br>1.343(4) | 1.367(4)<br>1.373(4)<br>1.369(5)<br>1.367(5) | 31.79<br>31.16 |

* Information is given for two independent units 1 and 2; formula is given without $C_6H_4Cl_2$ molecules

Further investigation of the crystal structure of **1** reveals that the $\{Fe^{II}(TI^{\bullet-})(TI^{2-})\}_2$ dimers form two-dimensional layers with channels available for accommodation of bulky {cryptand(K⁺)} cations (Fig. S5). There are several S···S approaches between TI units from different dimers of 3.67-3.68 Å length. However, those are only side-by-side approaches.

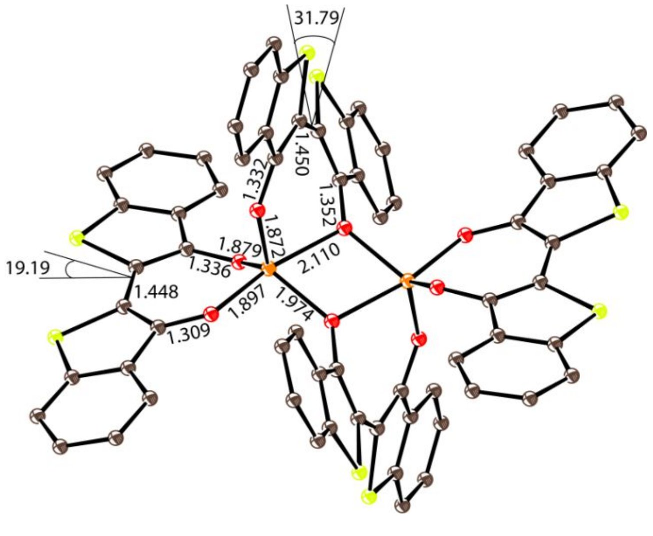

**Fig. 2** Geometry, bond length and some angles for one of two independent $\{Fe^{II}(TI^{\bullet-})(TI^{2-})\}_2$ dimers. Only half of the dimer is crystallographically independent. Geometry of another dimer is shown in Fig. S5. Carbon is brown, oxygen is red, iron is orange, and sulfur is yellow. Errors for the bond length are 0.002 Å for the O-Fe bonds, 0.004 Å for the C-O bonds, and 0.005 Å for the C-C bonds.

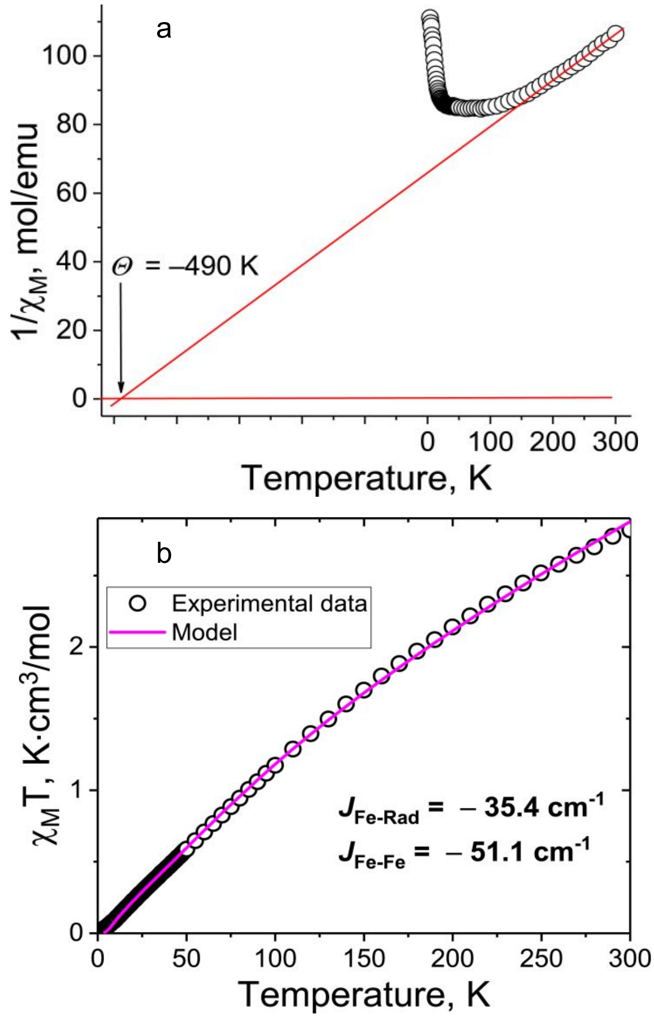

**Fig. 3** Magnetic data for compound **1**: (a) temperature dependence of reciprocal molar magnetic susceptibility of polycrystalline **1** and the determination of Weiss temperature; (b) fitting of the experimental data by the PHI program for the 4-spin system consisting of $TI^{\bullet-}$ ($S$ = 1/2) -$Fe^{II}$ ($S$ = 2) - $Fe^{II}$ ($S$ = 2) - $TI^{\bullet-}$ ($S$ = 1/2) coupled spins[9].

Magnetic properties of **1** were studied by SQUID and EPR techniques. EPR spectra for a polycrystalline sample of complex **1** shows an intense narrow asymmetric signal which can be fitted well by two lines with $g_1$ = 2.0021 and the linewidth ($\Delta H$) of 0.48 mT, and $g_2$ = 2.0025 and $\Delta H$ = 0.49 mT at room temperature (Fig. S6, spectrum at 272 K is shown) and can unambiguously be attributed to *cis*-$TI^{\bullet-}$ radical anions. Similar parameters of EPR signal were previously found for the radical anion {Crypt($Na^+$)}($TI^{\bullet-}$) salt[3g]. Integral intensity of this signal corresponds to the contribution of about one $S$ = 1/2 spin per $Fe^{II}(TI^{\bullet-})(TI^{2-})$ fragment. Any other signals including broad signals from paramagnetic Fe are not found in the high-temperature EPR spectrum of **1**, most probably due to short spin-lattice relaxation times for $Fe^{II}$ [7]. At the same time the contribution from $Fe^{II}$ should be rather small below 50K due to the antiparallel arrangement of $Fe^{II}$ spins in the dimers. Such behavior indicates the formation of even spin iron species and the absence of odd spin $Fe^{I}$ and $Fe^{III}$ but does not contradict with the presence of diamagnetic $TI^{2-}$. EPR signal from $TI^{\bullet-}$ supports the $\{Fe^0(TI^0)(TI^{\bullet-})\}^-$ and $\{Fe^{II}(TI^{\bullet-})(TI^{2-})\}^-$ configurations. Taking into account essential contribution to magnetic susceptibility from iron (that is not possible for $Fe^0$), only the $\{Fe^{II}(TI^{\bullet-})(TI^{2-})\}^-$ configuration with $Fe^{II}$ ($S$ = 2) can form in **1**. Structural data also support the formation of $\{Fe^{II}(TI^{\bullet-})(TI^{2-})\}^-$ due to the presence of TI with slightly different geometry. EPR signal from $TI^{\bullet-}$ in **1** shows nearly temperature independent parameters down to 50 K but below this temperature both lines are strongly broadened (up to 10 times), and $g$-factors of the lines are noticeably shifted to the opposite directions (Fig. S7). That indicates the inclusion of $TI^{\bullet-}$ in strong magnetic coupling of spins within the dimer. Integral intensity of EPR signal reaches maximum at 30 K and decreases strongly below this temperature (Fig. S8) indicating antiparallel arrangement of $TI^{\bullet-}$ spins within the dimer (as shown above).

Magnetic susceptibility of **1** has two contributions: from the Curie impurities (2.6% of $S$ = 1/2 spins per half of dimer) and from the $\{Fe^{II}(TI^{\bullet-})(TI^{2-})\}_2$ dimers which can be obtained after the subtraction of the Curie impurities contribution from the experimental data (Figs. 3b and S9). Crystal and magnetic data show that there are two high-spin (S = 2) iron(II) atoms linked by two bridging oxygen atoms belonging to diamagnetic $TI^{2-}$ dianions, and two $TI^{\bullet-}$ radical anions additionally coordinate to each iron(II) atom. As a result, four spin $TI^{\bullet-}$- $Fe^{II}$ - $Fe^{II}$ -$TI^{\bullet-}$ system is formed within each dimer. The $\chi_M T$ value for **1** is 2.82 emu·K·mol$^{-1}$ at 300 K per $Fe^{II}(TI^{\bullet-})(TI^{2-})$ fragment, and this value decreases even below 300 K. Calculated magnetic moment is 3.0 emu·K·mol$^{-1}$ per one high-spin iron(II) ($S$ = 2) and 3.37 emu·K·mol$^{-1}$ per system of non-interacting one $S$ = 1/2 spin from $TI^{\bullet-}$ and one high-spin iron(II) ($S$ = 2). It is seen that the observed value of 2.82 emu·K·mol$^{-1}$ is lower than the calculated value of 3.37 emu·K·mol$^{-1}$ and that can be explained by substantial antiferromagnetic coupling of spins. Indeed, Weiss temperature $\Theta$ = –490 K extracted from the 1/χ plot is very negative (Fig. 3a).

The susceptibility of the dimer was modeled using the program PHI[8]. The best fit (residual $R$ = 0.018) for the 4-spin system consisting of two $S$ = 1/2 and two $S$ = 2 spins yielded the exchange constants of $J(Fe^{II}\text{-}TI^{\bullet-})/k_B$ = –35.4 cm$^{-1}$ and $J(Fe^{II}\text{-}Fe^{II})/k_B$ = –51.1 cm$^{-1}$, as well as spin-orbital coupling parameter $\lambda$ = – 48.2 cm$^{-1}$ (–0.00598 eV), the combined orbital reduction value of $\sigma$ = 0.88 and $g$ = 2.04 for the two HS $Fe^{II}$ atoms, while $g$-factor for each of the radicals was fixed at $g$ = 2.0. The values obtained follow similar[9] coordination compounds and indicate that there is indeed a degree of SO interaction present[10] in the system. On the whole, the $\{Fe^{II}(TI^{\bullet-})(TI^{2-})\}_2$ dimers show strongly negative Weiss temperature and large exchange interactions. Nevertheless, the magnitude of those interactions in **1** are still smaller than those reported for other high-spin Fe(II) complexes[11]. That could be attributed to the nature of bridging ligand as well as the overall distance between the magnetic centers.

In order to evaluate interdimer interactions, the intermolecular overlap integrals were examined by the extended Hückel method[12] based on the refined crystal structure. The obtained overlap value of 0.2x10$^{-3}$ between frontier orbitals supports the assumption that coupling between the dimers is essentially lower than the intra-dimer one.

As a conclusion a complex of iron(II) has been obtained with anionic thioindigo ligands. That is a rare example of the coordination complex with differently charged ligands of the same chemical species. Oxygen atom of diamagnetic $TI^{2-}$ becomes a bridge between two iron(II) atoms and the $TI^{\bullet-}$ radical anions become end groups in the discrete species made of four $TI^{\bullet-}$ ($S$ = 1/2) - $Fe^{II}$ ($S$ = 2) - $Fe^{II}$ ($S$ = 2) - $TI^{\bullet-}$ ($S$ = 1/2) coupled spins. As a result, two types of distinct interactions are observed in the dimers: the first ones are in the $Fe^{II}$ - $Fe^{II}$ pairs and are described by the exchange value of ($J/k_B$ ($Fe^{II}$ - $Fe^{II}$) = –51.1 cm$^{-1}$ and the antiparallel arrangement of the $TI^{\bullet-}$ spins is occurring through the $Fe_2O_2$ unit with $J(Fe^{II}\text{-}TI^{\bullet-})/k_B$ = –35.4 cm$^{-1}$. Thus, organic radicals are involved in strong magnetic coupling of spins observed in the inorganic $Fe_2O_2$ subsystem. The study of other metal-dye magnetic systems is now in progress.

## Conflicts of interest

There are no conflicts to declare.

## Acknowledgements.

The work was supported by the Ministry of Science and Higher education of the Russian Federation (registration number AAAA-A19-119092390079-8) and by the Kyoto University Foundation and the JST (ACCEL) 27 (100150500019) project.

## Notes and references

‡Crystal data for **1**: $C_{112}H_{112}Fe_2Cl_4K_2N_4O_{20}S_8$, F.W. 2422.23, black block, 120(1) K, triclinic, $P\bar{1}$, $a$ = 14.2994(6), $b$ = 18.5793(6), $c$ = 23.5935(7) Å, $\alpha$ = 68.714(3), $\beta$ = 78.174(3), $\gamma$ = 73.182(3)°, $V$ = 5555.6(4) Å$^3$, $Z$ = 2, $d_{calcd}$ = 1.448 M gm$^{-3}$, $\mu$ = 0.653 mm$^{-1}$, $F(000)$ = 2516, $T$ = 120(2) K, $2\theta_{max}$ = 59.492°; 66054 reflections collected, 25979 independent; $R_1$ = 0.0687 for 14229 observed data [$> 2\sigma(F)$] with 740 restraints and 1499 parameters; $wR_2$ = 0.1359 (all data); final G.o.F. = 1.011. CCDC 1992136.

1 a) Handbook of textile and industrial dyeing, Ed. M. Clark, V. Principles, processes and type of dyes, Woodhead Publishing, 2011. ISBN 978-1-84569-695-5; (b) Dyes, General Survey, H. Mustroph, Ullmann's Encyclopedia of Industrial Chemistry. Wiley-VCH. 2014, DOI: 10.1002/14356007.a09_073. ISBN 3527306730.

2 (a) E. D. Głowacki, G. Voss and N. S. Sariciftci, *Adv. Mater*. 2013, **25**, 6783; (b) O. Pitayatanakul, T. Higashino, T. Kadoya, M. Tanaka, H. Kojima, M. Ashizawa, T. Kawamoto, H. Matsumoto, K. Ishikawa and T. Mori, *J. Mater. Chem. C,* 2014, **2**, 9311; (c) M. Yao, K. Kuratani, T. Kojima, N. Takeichi, H. Senoh and T. Kiyobayashi, *Sci. Rep*. 2014, **4**, 3650; (d) K.-Y. Law, *Chem. Rev.,* 1993, **93**, 449.

3 (a) W. Beck, C. Schmidt, R. Wienold, M. Steinmann and B. Wagner, *Angew. Chem. Int. Ed*., 1989, **28**, 1529; (b) J. -Y. Wu, C. -H. Chang, P. Thanasekaran, C.- C. Tsai, T.- W. Tseng, G. -H. Lee, S. -M. Peng and K.- L. Lu, *Dalton Trans*. 2008, 6110; (c) P. Mondal, M. Chatterjee, A. Paretzki, K. Beyer, W. Kaim and G. K. Lahiri, *Inorg. Chem*. 2016, **55**, 3105; (d) F. -S. Guo and R. A. Layfield, *Chem. Commun*. 2017, **53**, 3130; (e) W. Kaim and G. K. Lahiri, *Coord. Chem. Rev*. 2019, **393**, 1; (f) D. V. Konarev, S. S. Khasanov, A. V. Kuzmin, A. F. Shestakov, A. Otsuka, H. Yamochi, G. Saito and R.N. Lyubovskaya, *Dalton Trans.,* 2016, **45**, 17095; (g) D.V. Konarev, S. S. Khasanov, A. F. Shestakov, A. M. Fatalov, M. S. Batov, A. Otsuka, H. Yamochi, H. Kitagawa and R. N. Lyubovskaya, *Dalton Trans.,* 2017, **46**, 14365. (h) D. V. Konarev, A. V. Kuzmin, A. M. Fatalov, S.S. Khasanov, E. I. Yudanova and R. N. Lyubovskaya, *Chem. Eur. J.* 2018, **24**, 8415; (i) D. V. Konarev, L. V. Zorina, S. S. Khasanov, A. F. Shestakov, A. M. Fatalov, A. Otsuka, H. Yamochi, H. Kitagawa and R. N. Lyubovskaya, *Inorg. Chem*. 2018, **57**, 583.

4 (a) L. -S. R. Yeh and A. J. Bard, *J. Electroanal. Chem*., 1976, **70**, 157; (b). A. Roessler, D. Crettenand, O. Dossenbach, W. Marte and P. Rys, *Electrochimica Acta*, 2002, **47**, 1989.

5 D. V. Konarev, L. V. Zorina, S. S. Khasanov, A. Otsuka, H. Yamochi, H. Kitagawa, R. N. Lyubovskaya, *New J. Chem,* 2019, **43**, 7350.

6 H. von Eller, *Bull. Soc. Chim. Fr.,* 1955, **106**, 1438.

7 S. K. Misra, S. Diehl, D. Tipikin, and J. H. Freed, *J. Magn. Reson*. 2010, *205*, 14.

8 N. F. Chilton, R. P. Anderson, L. D. Turner, A. Soncini and K. S. Murray, *J. Comput. Chem*. 2013, **34**, 1164.

9 J. M. Zadrozny, S. M. Greer, S. Hill and D. E. Freedman, *Chem. Sci.* 2016, *7*, 416.

10 N. Russo, D. R. Salahub “Metal-Ligand Interactions: Structure and Reactivity”, *Springer*, 1996, pp. 139-162

11 S. Yogendra, T. Weyhermüller, A. W. Hahn and S. DeBeer, *Inorg. Chem.* 2019, **58**, 9358.

12 J. Ren, W. Liang and M. -H. Whangbo, Crystal and Electronic Structure Analysis Using CAESAR; Prime Color Software, Inc., 1998. Default parameters were used.

Communication

# Strong magnetic coupling of spins in Fe(II) dimers with differently charged thioindigo ligands

D.V. Konarev, A.V. Kuzmin, M.S. Batov, S.S. Khasanov, A. Otsuka, H. Yamochi, H. Kitagawa and R.N. Lyubovskaya

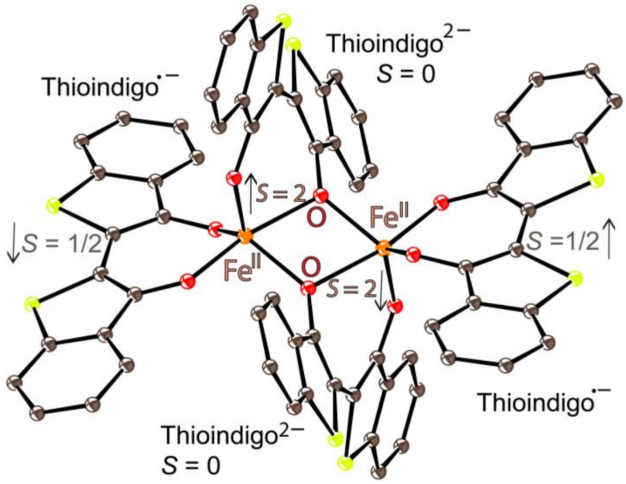

First coordination complex of iron(**II**) with both radical anion and dianion of thioindigo $\{\mathrm{Crypt[2.2.2](K^+)}\}_2\{\mathrm{Fe^{II}(TI^{\bullet-})(TI^{2-})}\}_2 \cdot 2\mathrm{C_6H_4Cl_2}$ (**1**) was obtained. Complex has two high-spin Fe$^{II}$ centers separated by two oxygen atoms, and two TI$^{\bullet-}$ radical anions are coordinated to each Fe$^{II}$ to form 4-spin system TI$^{\bullet-}$-Fe$^{II}$- Fe$^{II}$-TI$^{\bullet-}$ of coupling spins. Strong Fe$^{II}$- Fe$^{II}$ ($J/k_B$ = -51.1 K) and weaker Fe$^{II}$- TI$^{\bullet-}$ interactions ($J/k_B$ = -35.4 K) are observed in these chains.